Molecular Crystals and Liquid Crystals

ISSN: 1542-1406 (Print) 1563-5287 (Online) Journal homepage: http://www.tandfonline.com/loi/gmcl20

Synthesis of Poly(#-caprolactone) Grafted Poly(2-hydroxyethyl methacrylate) Functionalized Hydroxyapatite by RAFT and ROP

Xuan Thang Cao, Ali Md Showkat, Chan Park, Yeong Soon Gal & Kwon Taek Lim

To cite this article: Xuan Thang Cao, Ali Md Showkat, Chan Park, Yeong Soon Gal & Kwon Taek Lim (2015) Synthesis of Poly(#-caprolactone) Grafted Poly(2-hydroxyethyl methacrylate) Functionalized Hydroxyapatite by RAFT and ROP, Molecular Crystals and Liquid Crystals, 618:1, 103-110, DOI: 10.1080/15421406.2015.1076299

To link to this article: http://dx.doi.org/10.1080/15421406.2015.1076299

Published online: 07 Oct 2015.

Mol. Cryst. Liq. Cryst., Vol. 618: pp. 103–110, 2015

ISSN: 1542-1406 print/1563-5287 online
DOI: 10.1080/15421406.2015.1076299

Synthesis of Poly(ε-caprolactone) Grafted Poly(2-hydroxyethyl methacrylate) Functionalized Hydroxyapatite by RAFT and ROP

XUAN THANG CAO,[1] ALI MD SHOWKAT,[1] CHAN PARK,[2] YEONG SOON GAL,[3] AND KWON TAEK LIM[1,*]

[1]Department of Imaging System Engineering, Pukyong National University, Busan, Korea
[2]Department of Materials Engineering, Pukyong National University, Busan, Korea
[3]Polymer Chemistry Laboratory, College of Engineering, Kyungil University, Gyeongsan, Gyeongsangbuk-Do, South Korea

Poly(ε-caprolactone) grafted poly(2-hydroxyethyl methacrylate) functionalized hydroxyapatite (HAP@PHEMA-g-PCL) nanocomposites were synthesized by the combination of reversible addition fragmentation chain transfer (RAFT) polymerization and ring-opening polymerization (ROP). The RAFT agent was anchored on the surface of hydroxyapatite nanocrystals (HAPs) through the silane condensation process of 3-chloropropyltrimethoxysilane followed by reaction with potassium xanthogenate. Poly(2-hydroxyethyl methacrylate) (PHEMA) was covalently functionalized on the surface of HAPs by RAFT polymerization. Then, poly(ε-caprolactone) (PCL) was grafted on HAPs by ROP based on the hydroxyl groups of PHEMA to afford HAP@PHEMA-g-PCL. The structure and composition of HAP@PHEMA-g-PCL nanocomposites were characterized by FT-IR, XRD, and TGA analyses. The morphology and formation of the polymer encapsulating HAPs were demonstrated from SEM and TEM images, while the ^{1}H MNR analysis of the cleaved PHEMA-g-PCL confirmed the grafting.

Keywords Hydroxyapatite; 2-hydroxyethyl methacrylate; ε-caprolactone; RAFT; ROP

1. Introduction

Hydroxyapatite nanocrystals (HAPs) have attracted much attention due to its chemical and biological similarity to mammalian bone, which has shown great promise in a wide range of applications in academia, industry, and medicine [1-3]. However, either in block or granular forms pure HAPs could not degrade in the human body [4,5]. Therefore, an ideal type of HAPs is required to meet the demands in both biological characteristics and mechanical

*Address correspondence to Kwon Taek Lim, Department of Imaging System Engineering, Pukyong National University, 599-1 Daeyeon 3-Dong, Nam-Gu, Busan 608-737, Korea (ROK). E-mail: ktlim@pknu.ac.kr

Color versions of one or more of the figures in the article can be found online at www.tandfonline.com/gmcl.

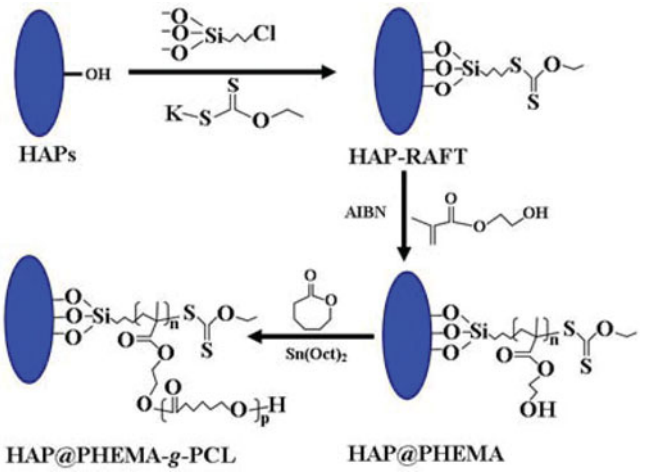

Scheme 1. Schematic representation for synthesis of HAP@PHEMA-g-PCL.

properties. The introduction of polymer moieties to the backbone of HAPs has been found to improve the physicochemical properties of HAPs, such as solubility, and gives rise to some interesting synergistic characteristics for use in drug delivery and tissue engineering. Encapsulating HAP by a biocompatible polymer is one of the best adopted approaches to solve the existing impediment.

Poly(2-hydroxyethyl methacrylate) (PHEMA) is well known hydrogel. The PHEMA has excellent properties such as biodegradability, biocompatible, and non-toxicity and has been used for drug release and artificial skin [6-8]. Besides, poly(ε-caprolactone) (PCL) is a biocompatible and hydrophobic polymer with potential applications for bone and nerve tissue engineering [9,10]. Recently, biodegradable PCL grafted PHEMA copolymers were synthesized for antitumor nanocarrier applications [11].

In this work, we synthesized poly(ε-caprolactone) grafted poly(2-hydroxyethyl methacrylate) functionalized hydroxyapatite (HAP@PHEMA-g-PCL) nanocomposites by the combination of reversible addition fragmentation chain transfer (RAFT) polymerization and ring-opening polymerization (ROP) through "grafting from" strategy (Scheme 1).

2. Experimental Methods

2.1. Materials

All chemicals used for the experiments were purchased from Sigma-Aldrich. 2-Hydroxyethyl methacrylate (HEMA) and ε-caprolactone (ε-CL) were passed through an alumina column and distilled under reduced pressure before use. 2,2'-Azobisisobutyronitrile (AIBN) was recrystallized with ethanol before use. HAPs were supplied by the Display and Lighting Phosphor Bank at Pukyong National University. 3-Chloropropyl-trimethoxysilane (CTS), potassium xanthogenate, stannous octoate ($Sn(Oct)_2$), and solvents of analytical grade were used as received.

2.2. Immobilization of the RAFT Agent onto HAPs (HAP-RAFT)

In a typical experiment, 1.6 g of dried HAPs, 9 mL of toluene, and 0.5 mL of distilled water were put into a 100 mL three-neck round bottom flask, and the mixture was sonicated in a bath for 30 min. Then, 3.0 mL of CTS was added into the solution and stirred at 80°C for 12 h. The product HAP-Cl was filtered and washed sequentially with toluene (2 × 20 mL) and methanol (2 × 15 mL). After drying under vacuum at 40°C overnight, 1.25 g of HAP-Cl was placed into a 50 mL of potassium xanthogenate solution, and stirred for 12 h at 70°C under nitrogen. At the end of the reaction, the product was filtered and washed with anhydrous ethanol three times. The RAFT agent functionalized HAPs (HAP-RAFT) was dried in a vacuum oven at 40°C for 24 h.

2.3. Synthesis of HAP@PHEMA-g-PCL Composites

Poly(2-hydroxyethyl methacrylate) functionalized hydroxyapatite (HAP@PHEMA) composites were prepared as follows: 0.2 g of HAP-RAFT, 2.0 g of HEMA, 0.02 g of AIBN, 2 mL of anhydrous DMF, and a Teflon-coated stir bar were placed in a 25 mL round bottom flask equipped with a reflux condenser. The solution was purged under nitrogen, and stirred at 70°C for 12 h. The product was purified by precipitating in diethyl ether, washed with DMF, and dried under vacuum at 40°C overnight. For HAP@PHEMA-g-PCL, 0.1 g of HAP@PHEMA was dispersed into 5 mL of anhydrous DMF in a round bottom flask. Then, ε-CL (0.5 g) and deoxygenate $Sn(Oct)_2$ (10 mg) were added to the solution by a syringe and stirred for 4 h at 110°C under nitrogen. The resulting solution was diluted into DMF, and precipitated in diethyl ether. Finally, the product was dried under vacuum at 40°C for 24 h. PHEMA-g-PCL chains were cleaved from HAP@PHEMA-g-PCL for identification of the grafted PHEMA-g-PCL. In brief, 100 mg of HAP@PHEMA-g-PCL was dissolved in a mixture of 1 mL of HCl (2 M) and 10 mL of DMF. The solution was stirred for 24 h. The cleaved PHEMA/PCL in the organic layer was precipitated in diethyl ether and dried in vacuum at 40°C for 24 h.

2.4. Instrumentation

The bonding nature in the as-prepared composites was recorded by fourier transformed infrared spectrophotometry (FT-IR) using a BOMEM Hartman & Braun FT-IR. Thermogravimetric analysis (TGA) was conducted with a Perkin-Elmer Pyris 1 analyzer (USA). The crystallographic state of the nanocomposites was studied by a Philips X'pert-MPD system diffractometer. ^{1}H NMR spectra were recorded on a JNM-ECP 400 (JEOL) instrument using DMSO-d_6 solvent. Transmission electron microscopy (TEM) images were recorded using a Hitachi H-7500 instrument operated at 80 kV. The morphology analyses of the hybrids were carried out by using scanning electron microscopy (SEM) images equipped with an energy dispersive X-ray (EDX) spectrometer (Hitachi JEOL-JSM-6700F system, Japan).

3. Results and Discussion

FT-IR spectroscopy studies were examined to confirm the structure of HAPs and composites. The spectrum of HAPs (Figure 1a) shows strong absorption bands at 475-633 cm^{-1} and 1037-1091 cm^{-1} ranges which are assigned to the vibrations of O-P-O framework bonds. The broad band at 3400 cm^{-1} implied the vibration of -OH stretching. The silica network is anchored on HAPs surface by Si-O bonds. This absorbance band is supposed

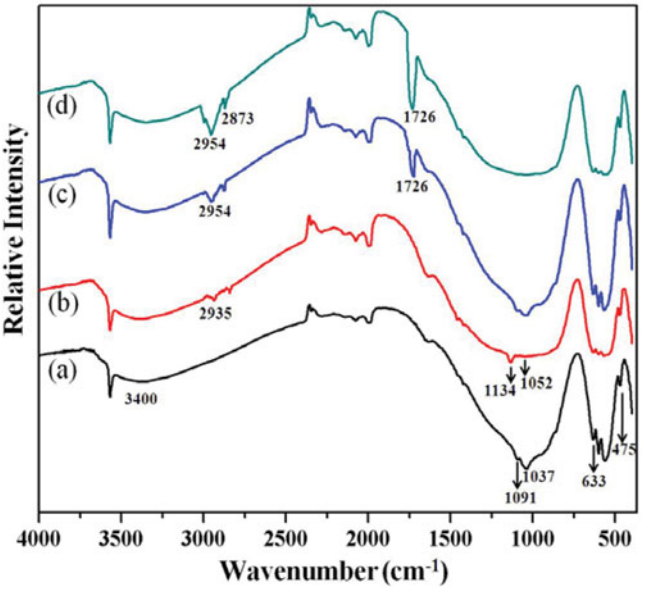

Figure 1. FT-IR spectra of (a) pure HAPs, (b) HAP-RAFT, (c) HAP@PHEMA, and (d) HAP@PHEMA-g-PCL composites.

to appear at ~586 cm^{-1} but due to overlapping with O-P-O vibration band of HAPs, it cannot be seen independently in the FT-IR spectrum (Figure 1b). However, the C-H stretching vibration of RAFT moieties is shown at 2935 cm^{-1}. After incorporation of potassium xanthogenate into HAP-Cl, the resulting HAP-RAFT is formed via covalent bonding as indicated by the two characteristic absorption bands at 1052 and 1134 cm^{-1} which are mainly due to the stretching vibration of C=S and C-O moieties, respectively (Figure 1b). The new peaks appear at 1726 and 2954 cm^{-1} in the spectrum of HAP@PHEMA (Figure 1c), which are attributed to carbonyl and methylene group respectively, indicating that PHEMA was grafted on HAPs. In addition, ε-CL was polymerized by the ring-opening reaction based on the hydroxyl group of PHEMA. The spectra of HAP@PHEMA-g-PCL (Figure 1d) and HAP@PHEMA (Figure 1c) show the peaks in the same position at 1726 and 2954 cm^{-1} correspond to the C=O and CH_2 bond stretching vibrations. The former peak intensities are stronger than the latter one due to the enhancement of C=O and CH_2 group in PCL chains. The FT-IR result reveals PCL is grafted onto HAP@PHEMA composites.

The crystal and physical changes of HAPs, HAP@PHEMA, and HAP@PHEMA-G-PCL were investigated by XRD analysis. All the peaks of the HAP@PHEMA (Figure 2b), and HAP@PHEMA-g-PCL (Figure 2c) are perfectly indexed to crystalline HAPs with 2θ values of 25.9°, 29.0°, 31.8°, 32.9°, 34.1°, 39.8°, 46.7°, 49.5°, 50.5°, 51.2°, 52.1°, 53.2°, 64.2°, and 65.0° correspond to the crystal planes of (002), (210), (211), (300), (202), (310), (222), (213), (321), (410), (402), (004), (323), and (511), respectively (Figure 2a). The XRD results demonstrate the grafting of polymers does not alter the crystallinity of HAPs.

TGA analysis was performed in the temperature range from 50 to 800°C to determine the amount of organic components immobilized onto HAPs, and the results are shown in Figure 3. It is observed that HAPs lose about 1.7% of their total weight because of the removal of adsorbed water (Figure 3a). After the modification of HAPs, the weight

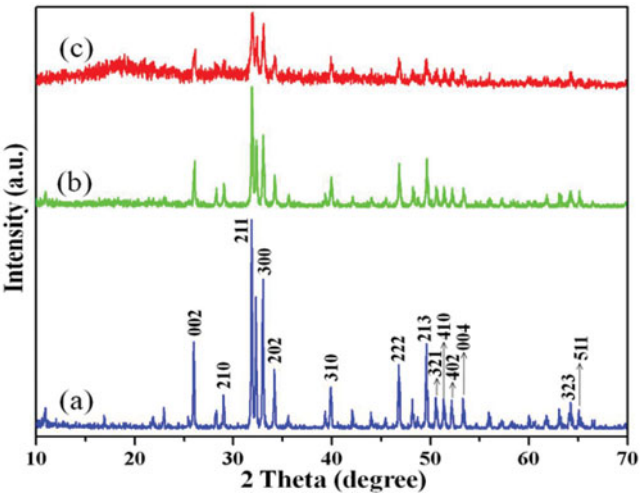

Figure 2. XRD patterns of (a) HAPs, (b) HAP@PHEMA, and (c) HAP@PHEMA-g-PCL.

loss is due to the decomposition of organic components. The weight loss of the HAP-RAFT is 6.1% in the whole temperature range due to the thermal degradation of the RAFT agent (Figure 3b). The HAP@PHEMA and HAP@PHEMA-g-PCL start to decompose at 300°C, and their weight loss are 23% and 37.2% at 800°C, respectively (Figure 3c and d). The TGA curve of cleaved PHEMA-g-PCL shows that the weight loss is 95% at 430°C (Figure 3e). Therefore, the presence of HAPs in the composites enhanced the thermal stability.

The ^{1}H NMR spectrum of polymers cleaved from HAPs provided further evidence for the formation of PHEMA-g-PCL (Figure 4). The signals at 1.09, 1.88, and 3.98 ppm are

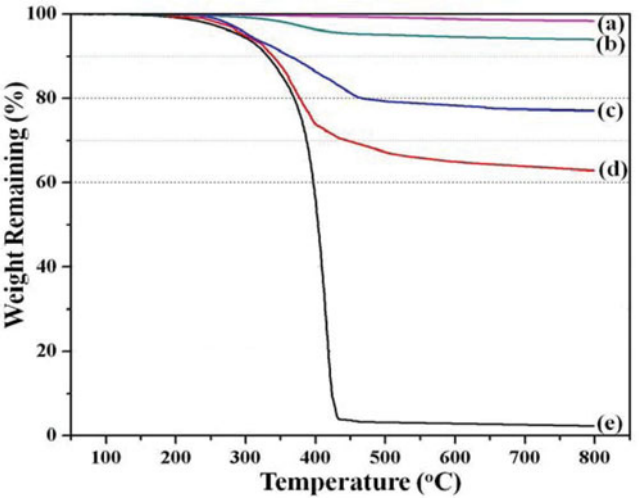

Figure 3. TGA spectra of (a) HAPs, (b) HAP-RAFT, (c) HAP@PHEMA, (d) HAP@PHEMA-g-PCL, and (e) cleaved PHEMA-g-PCL.

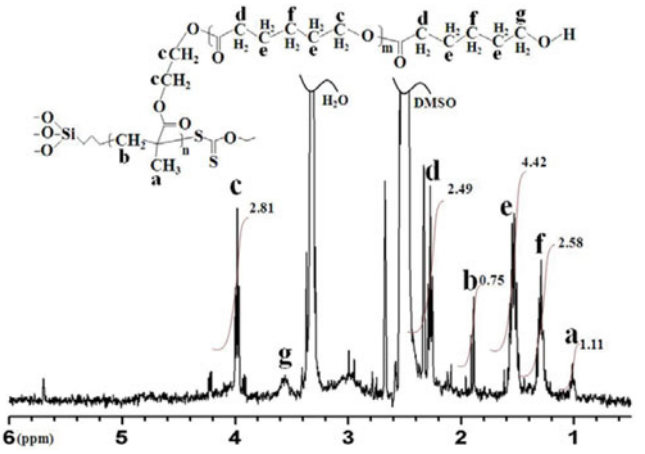

Figure 4. [1]H NMR spectrum of the cleaved PHEMA-g-PCL in DMSO-d_6.

assigned to the proton a, b, and c in the PHEMA moiety, respectively. The characteristic peaks for the PCL pendent at 1.29, 1.52, 2.27, and 3.56 ppm are ascribed to the protons f, e, d, and g, respectively. The result indicated PHEMA-g-PCL polymers were immobilized on HAPs.

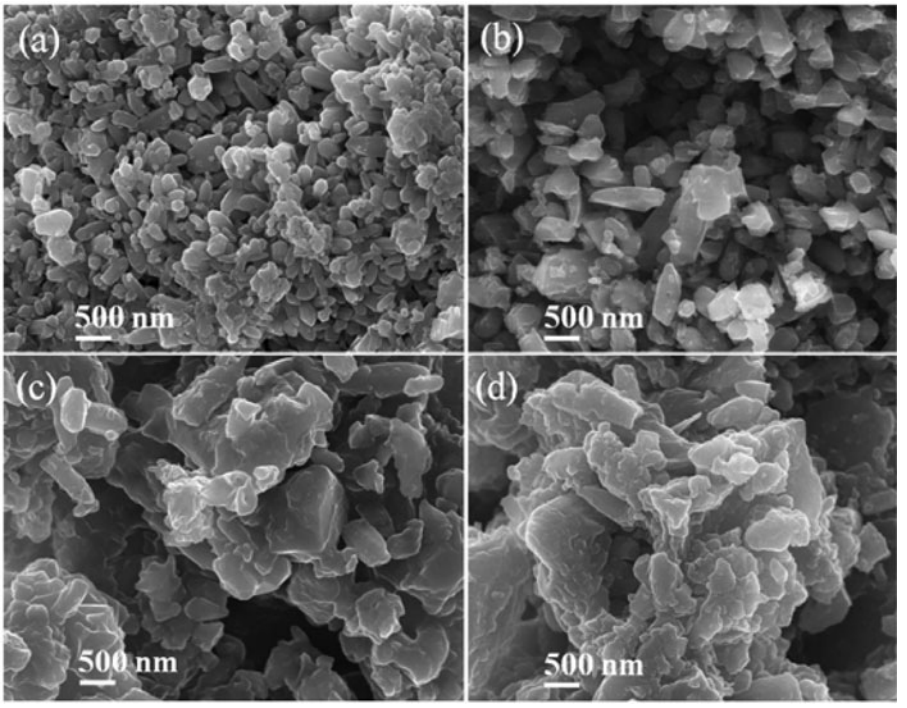

Figure 5. SEM images of (a) HAPs, (b) HAP-RAFT, (c) HAP@PHEMA, and (d) HAP@PHEMA-g-PCL.

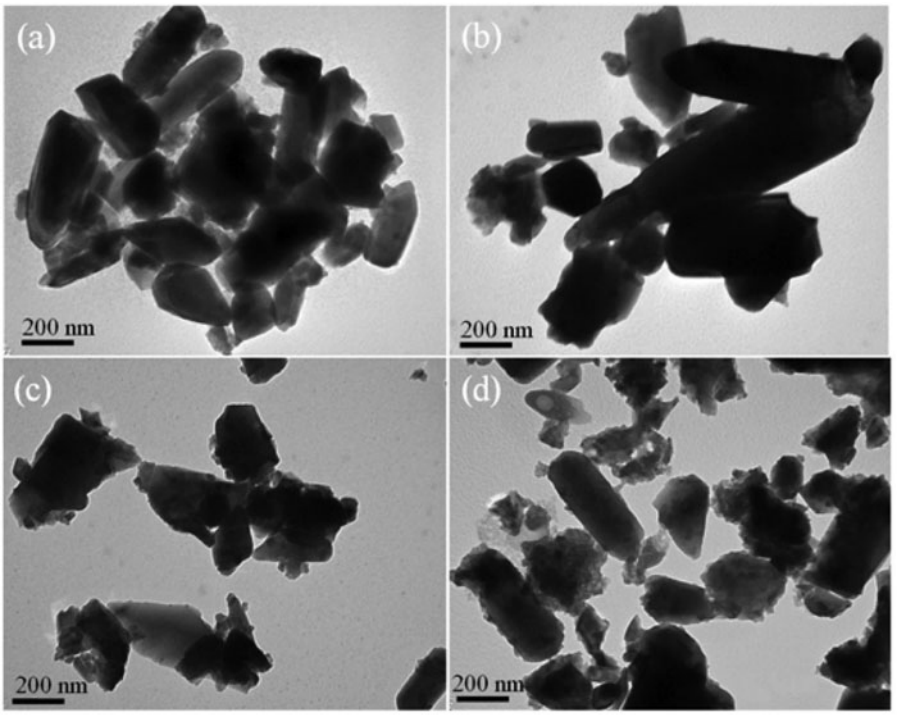

Figure 6. TEM images of (a) HAPs, (b) HAP-RAFT, (c) HAP@PHEMA, and (d) HAP@PHEMA-g-PCL.

Figure 5 shows the typical SEM images of the HAPs and as-synthesized composites. The morphology of HAPs displays distinct particles as shown in Figure 5a. The shape of HAP-RAFT was slightly different from pure HAPs, indicating the immobilization of the RAFT agent (Figure 5b). After RAFT polymerization, the shape of HAPs was significantly changed. The shape of nanocrystals became larger and irregular (Figure 5c) due to the grafting of the PHEMA polymer. Furthermore, the grafting of PCL exhibited the morphology of nanocrystals which nestled closely because of the coverage of PCL grafted chains (Figure 5d).

TEM micrographs of HAPs and composites in methylene chloride are showed in Figure 6. It is observed that HAPs (Figure 6a) and HAP-RAFT (Figure 6b) particles are dramatically agglomerated. After the modification, the surface of HAPs was covalently wrapped with polymer chains lead to the formation of HAP@PHEMA (Figure 6c) and HAP@PHEMA-g-PCL (Figure 6d), which were well dispersed. It might be due to the reduced surface energy originated from steric hindrance between HAPs.

4. Conclusion

The HAP@PHEMA-g-PCL composites were synthesized by the combination of RAFT polymerization and ROP technique. The structure of composites was confirmed by FT-IR analysis, and 1H NMR revealed the formation of PHEMA-g-PCL brushes on the surface of HAPs. The XRD results demonstrated that the crystallinity of HAPs was not damaged after grafting of the polymers. There was enhancing in the thermal stability of PHEMA-g-PCL

with the presence of HAPs in the composites as indicated by TGA. The SEM analysis showed that HAPs were wrapped with PHEMA-g-PCL, while TEM images illustrated a better dispersion of the composites in methylene chloride.

Funding

This work was supported by a Research Grant of Pukyong National University (2015Year)

References

[1] Wang, S., Wang, X., Xu, H., Abe, H., Tan, Z., Zhao, Y., Guo, J., Naito, M., Ichikawa, H., & Fukumori, Y. (2010). *Adv. Powder Technol.*, *21*, 268.
[2] Tabrizi, B. N., Fahami, A., & Kahrizsangi, R. E. (2014). *J. Ind. Eng. Chem.*, *20*, 245.
[3] Castillo, N. A. M., Ramos, R. L., Ortega, E. P., Perez, R. O., Cano, J. V. F., & Mendoza, M. S. B. (2014). *J. Ind. Eng. Chem.*, *20*, 4014.
[4] Deng, X., Hao, J., & Wang, C. S. (2011). *Biomaterials*, *22*, 2867.
[5] Thamaraiselvi, T. V., & Rajeswari, S. (2004). *Trends Biomater. Artif. Organs.*, *18*, 9.
[6] Arıca, M. Y., Bayramoglu, G., Arıca, B., Yalcın, E., Ito, K., & Yagci, Y. (2005). *Macromol. Biosci.*, *5*, 983.
[7] Ma, X., Wang, H., Jin, S., Wu, Y., & Liang, X. J. (2012). *Int. J. Nanomed.*, *7*, 1313.
[8] Prasitsilp, M., Siriwittayakorn, T., Molloy, R., Suebsanit, N., Siriwittayakorn, P., & Veeranondha, S. (2003). *J. Mater. Sci-Mater M.*, *14*, 595.
[9] Mobarakeh, L. G., Prabhakaran, M. P., Morshed, M., Esfahani, M. H. N., & Ramakrishna, S. (2010). *Mat. Sci. Eng. C-Bio. S.*, *30*, 1129.
[10] Annabi, N., Fathi, A., Mithieux, S. M., Weiss, A. S., & Dehghani, F. (2011). *J. Supercrit. Fluid.*, *59*, 157.
[11] Cheng, R., Wang, X, Chen, W., Meng, F, Deng, C., Liu, H., & Zhong, Z. (2012). *J. Mater. Chem.*, *22*, 11730.